

Statistical Analysis of the Correlation between Active Galactic Nuclei and Ultra-High Energy Cosmic Rays

Hang Bae Kim^{1,2*} and Jihyun Kim^{1†}

¹*Department of Physics and The Research Institute of Natural Science,
Hanyang University, Seoul 133-791, Korea and*

²*Korean Institute of Advanced Study (KIAS), Seoul 130-722, Korea*

We develop the statistical methods for comparing two sets of arrival directions of cosmic rays in which the two-dimensional distribution of arrival directions is reduced to the one-dimensional distributions so that the standard one-dimensional Kolmogorov-Smirnov test can be applied. Then we apply them to the analysis of correlation between the ultra-high energy cosmic rays (UHECR) with energies above 5.7×10^{19} eV, observed by Pierre Auger Observatory (PAO) and Akeno Giant Air Shower Array (AGASA), and the active galactic nuclei (AGN) within the distance 100 Mpc. For statistical test, we set up the simple AGN model for UHECR sources in which a certain fraction of observed UHECR are originated from AGN within a chosen distance, assuming that all AGN have equal UHECR luminosity and smearing angle, and the remaining fraction are from the isotropic background contribution. For the PAO data, our methods exclude not only a hypothesis that the observed UHECR are simply isotropically distributed but also a hypothesis that they are completely originated from the selected AGN. But, the addition of appropriate amount of isotropic component either through the background contribution or through the large smearing effect improves the correlation greatly and makes the AGN hypothesis for UHECR sources a viable one. We also point out that restricting AGN within the distance bin of 40–60 Mpc happens to yield a good correlation without appreciable isotropic component and large smearing effect. For the AGASA data, we don't find any significant correlation with AGN.

PACS numbers: 98.70.Sa

Keywords: cosmic rays, active galactic nuclei, angular correlation

* hbkim@hanyang.ac.kr

† jihyunkim@hanyang.ac.kr

I. INTRODUCTION

The sources of ultra-high energy cosmic rays (UHECR) still remain in veil, but the recent observation of the suppression in the energy spectrum of UHECR above the so-called Greisen-Zatsepin-Kuzmin (GZK) cutoff ($E_{\text{GZK}} \sim 4 \times 10^{19}$ GeV) [1, 2] indicates that at least the UHECR with energies above the GZK cutoff come from relatively close (within the GZK radius ~ 100 Mpc) extragalactic sources. The magnitude and extension of the intergalactic magnetic fields are supposed not to be large enough to significantly alter the arrival directions of UHECR with these energies. Thus, the distribution of arrival directions is correlated with the distribution of the sources and the arrival direction analysis for the UHECR with energies above the GZK cutoff can be very useful in identifying their sources. An important step toward this direction was initiated by the correlation between arrival directions of UHECR and nearby active galactic nuclei (AGN) reported by the Pierre Auger Observatory (PAO) [3]. Though further analysis with more data weakened the significance of the correlation [4, 5], it still remains as an important issue. Another important clue for the UHECR sources may come from the study of the correlation between the UHECR arrival directions and the large scale structures manifested in the galaxy distribution or the matter distribution. It was studied by several groups [5–10] and the results are not quite conclusive yet. The positive result will provide the basis for the further study of correlations between the UHECR and specific classes of astrophysical objects.

For the study of correlation between the arrival directions of UHECR and some astrophysical objects, we have to rely on the statistical methods. This is because the current limit of angular resolution in CR experiments and a poor understanding of the intergalactic magnetic fields make it difficult to pin down individual sources of UHECR from their arrival directions. This also seems to be unavoidable as we consider that currently the number of astrophysical objects which are candidates for UHECR sources is very large while the number of observed UHECR events is small yet.

Statistical studies of correlation between the arrival directions of UHECR and the astrophysical objects was done in many ways [3–5, 11–19]. In this paper, first we improve the previously used methods and combine them to obtain more reliable estimates of the significance of correlation. Our improvement is twofold. Firstly, while the previous analyses compared the *representative values* of the two-dimensional distributions of UHECR arrival directions, for example the number of UHECR events within the certain angular distance from the supposed sources, ours compares the *one-dimensional distributions* obtained from the two-dimensional distributions, which conveys more information in the sense that, compared with the above example of representative value, this one-dimensional distribution contains information about the number of UHECR events within any angular distance, not just within a certain specific angular distance. Secondly, the previous analyses focused on the deviation from isotropy rather than the direct correlation with the supposed sources by taking as their null hypothesis that the UHECR arrival directions are isotropically distributed. Here, we take as a null hypothesis the explicit source model for UHECR including the isotropic component and focus on the direct correlation of UHECR with the supposed sources. The basic idea is that we reduce the two-dimensional distribution of arrival directions to the one-dimensional distributions, which can be compared by using the well-known Kolmogorov-Smirnov (KS) test. Then, we apply these methods to examine the correlation between UHECR arrival directions and AGN. For statistical test, we set up the simple AGN model for the UHECR sources, in which all or a fraction of UHECR above a certain en-

ergy cutoff are originated from the AGN within a certain distance cut. For simplicity, we assume that all selected AGN have the equal luminosity and smearing angle of UHECR. The remaining fraction is filled with the isotropic component of UHECR to account for the contribution from the outside of the distance cut. We use the AGN data listed in the 12th edition of Véron-Cetty and Véron catalog [20] and the UHECR data obtained by PAO [4] and Akeno Giant Air Shower Array (AGASA) [21] to cover both the southern and northern hemispheres and compare the results drawn from them.

This paper is organized as follows. In section II, we introduce three statistical methods for comparing two distributions of arrival directions. In section III, we explain the simple AGN model for the UHECR sources and the details needed for the generation of Monte-Carlo events for the model and the statistical comparison with the observed data. Section IV presents the results of our analysis. We conclude in section V.

II. STATISTICAL COMPARISON OF TWO ARRIVAL DIRECTION DISTRIBUTIONS

We want to measure the correlation between the observed UHECR arrival directions and the directions of the candidate point sources to examine how plausible the candidate sources are. What we actually obtain through statistical analysis is the probability that the observed UHECR arrival direction distribution come from the expected UHECR arrival direction distribution from a given hypothesis about the sources. This comes from statistical comparison of two arrival direction distributions. Quantifying how similar two distributions of objects on the sphere are is a non-trivial problem. Various methods have been discussed [6, 8–10, 17, 18, 22–30]. Because the distribution on the sphere is two dimensional, we may apply the two-dimensional version of KS test [22, 31, 32]. The drawback of naive two-dimensional KS test is that it does not properly care the rotational symmetry that the distribution on the sphere has [33–35]. In this paper, we adopt the strategy that we reduce the two-dimensional distribution on the sphere to one-dimensional one for which the rotational symmetry is kept manifestly and apply the one-dimensional KS test to quantify the probability. For the reduction of the distribution on the sphere to one-dimensional distribution, we consider three ways described below.

A. Correlational Angular Distance Distribution

This is most useful when we consider the set of point sources for UHECR. By the correlation between two different sets of objects, we mean that nearby each object of one set, we can find objects of the other set at a certain level. To quantify the distance on the sphere, we use the angular distance θ between two objects on the sphere which is the angle between two unit vectors $\hat{\mathbf{r}}$ and $\hat{\mathbf{r}}'$ pointing two objects, that is, $\cos \theta = \hat{\mathbf{r}} \cdot \hat{\mathbf{r}}'$. For each object of the reference set, say the point source set, we count the number of objects of the other set, say the UHECR arrival direction set, within a certain angular distance θ . Then we sum up counts over all objects of the reference set and estimate the significance level of this number. This way of counting has been used previously in many literature [3, 4, 16, 23].

To quantify the significance level of the correlation, we need to know the probability distribution of the expected number of objects. It can be calculated analytically or obtained by Monte-Carlo simulation, once a hypothesis about the UHECR sources is set up. The simple

test bed is a hypothesis that the UHECR arrival directions are isotropically distributed. Then the correlation between the set of sources and the set of UHECR arrival directions was claimed based on that we observe more count of UHECR than that expected in the simple isotropic distribution. But what this procedure actually proves is that the observed UHECR arrival directions are not isotropically distributed. To make a stronger claim than simply something more than isotropy we should use an elaborated hypothesis for the test.

The above idea can be slightly generalized to estimate the significance level of the correlation between two sets of objects on the sphere. Instead of fixing the angular distance θ to a certain value, we consider the distribution of the count over the whole range of the angular distance, that is, from 0° to 180° . We call it the correlational angular distance distribution (CADD):

$$\text{CADD} : \{ \cos \theta_{ij'} \equiv \hat{\mathbf{r}}_i \cdot \hat{\mathbf{r}}'_j \mid i = 1, \dots, N; j = 1, \dots, M \}, \quad (1)$$

where $\hat{\mathbf{r}}_i$ are the UHECR arrival directions, $\hat{\mathbf{r}}'_j$ are the reference directions, and N and M are total numbers of them, respectively. In FIG. 1, we illustrate the basic idea and the usage of the CADD. We compare the CADD obtained from the reference set (presumably the set of point sources) and the observed UHECR arrival directions with that obtained from the same reference set and the simulated UHECR arrival directions from a given hypothesis. Because two distributions to be compared are one-dimensional, the KS test can be applied to yield the probability that the observed distribution of arrival directions comes from the hypothesis. The advantage of this method is that it is very simple in practice and does not require arbitrary angular binning. Listing in ascending order of all angular distances between pairs of objects in the reference set and the UHECR arrival direction set directly gives the cumulative probability distribution of the count number which is used in the KS test. Since we directly deal with the cumulative probability distribution, binning in angular distance is unnecessary and the expected cumulative probability distribution from the hypothesis can be made accurate simply by increasing the number of simulated events enough.

B. Flux Exposure Value Distribution

Koers and Tinyakov proposed another method to test the correlation between the sources and the observed UHECR [8]. In this method, the two-dimensional distribution of UHECR arrival directions is reduced to the one-dimensional distribution of expected flux values at UHECR arrival directions. At a given arrival direction, the expected flux value is the product of the UHECR flux expected from a given hypothesis for the sources and the exposure function at that direction. Thereby, we call it the flux exposure value distribution (FEVD):

$$\text{FEVD} : \{ F_i \equiv f(\hat{\mathbf{r}}_i)h(\hat{\mathbf{r}}_i) \mid i = 1, \dots, N \}, \quad (2)$$

where $\hat{\mathbf{r}}_i$ are the UHECR arrival directions, N is the total numbers of UHECR, $f(\hat{\mathbf{r}}_i)$ and $h(\hat{\mathbf{r}}_i)$ are the UHECR flux and the exposure function, respectively. It is also very simple in practice and does not require arbitrary angular binning. One additional merit of this method is that it can be used for the continuous source distribution. For the detailed motivations and merits of this method, see Ref. [8]. Here, we take this method for checking and comparison.

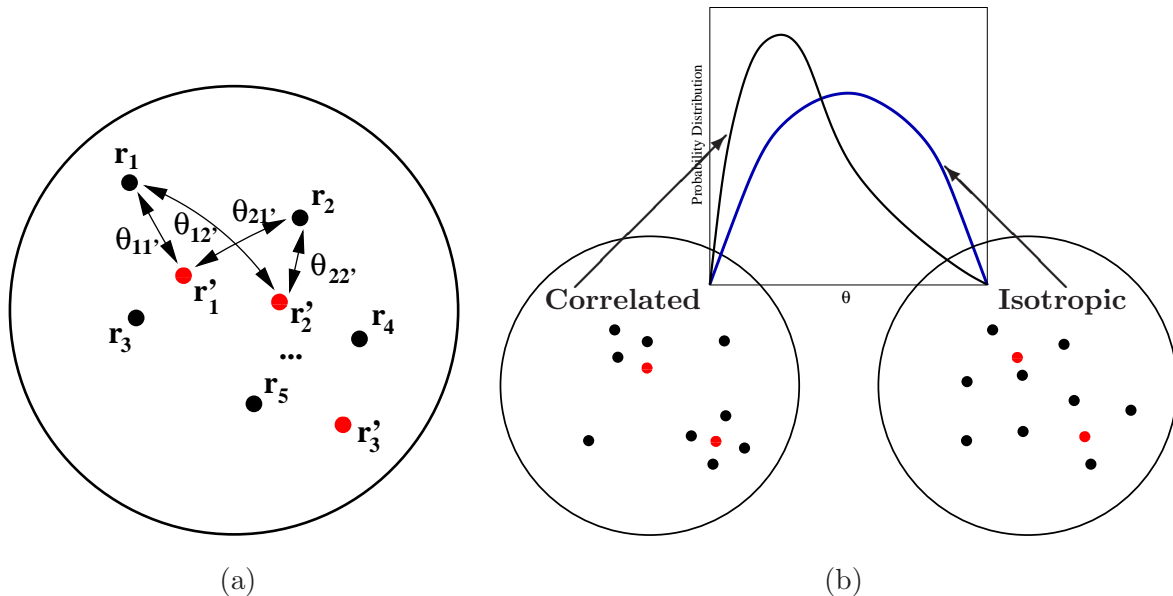


FIG. 1. Illustrations showing the basic idea of comparing CADD. (a) CADD is the distribution of all angular distances between the reference directions (red dots) and the UHECR arrival directions (black dots). (b) When the observed UHECR events are more clustered around the reference directions than, say, those of the isotropic distribution, the observed CADD has more counts at small angles than that expected from the isotropic distribution.

C. Auto-Angular Distance Distribution

The CADD and the FEVD with the one-dimensional KS test respects the rotational symmetry. But they reduce a two-dimensional distribution on the sphere to one-dimensional distribution of angular distances and flux values. It means that the loss of information occurs. The one-dimensional KS test on the CADD catches the correlation of the source directions and the CR directions, but it can be faked by, say, the aggregation of UHECR themselves around a few point sources. To compensate for this, we may consider the distribution of the angular distances of all pairs of UHECR arrival directions, which we call the auto-angular distance distribution (AADD):

$$\text{AADD} : \{ \cos \theta_{ij} \equiv \hat{\mathbf{r}}_i \cdot \hat{\mathbf{r}}_j \mid i, j = 1, \dots, N \}, \quad (3)$$

where $\hat{\mathbf{r}}_i$ are the UHECR arrival directions and N is the total numbers of UHECR. It catches the aggregation or spreading of UHECR arrival directions. It was used previously to examine the clustering of CR arrival directions [36–39]. The AADD method may not be so relevant for the correlation analysis because it does not measure the correlation directly. However, it is still useful to compare two distributions of arrival directions, and to test the hypothesis for the sources. It is quite useful when the number of sources is small or a few strong sources dominate over the others.

III. MODELING THE ARRIVAL DIRECTIONS OF UHECR

For a statistical test, we need to know the expected distribution of UHECR arrival directions. To get the expected distribution from a given model for the UHECR sources, Monte-Carlo simulation is commonly used. In this section, we present some details needed for the generation of UHECR arrival directions by using Monte-Carlo simulation and statistical comparison with the observed data.

A. Arrival directions of UHECR

For statistical analysis of arrival directions, we use the UHECR data reported by PAO [4] and by AGASA [21]. These data sets were selected with certain energy cuts. The energy cuts of the reported data sets are 5.7×10^{19} eV for the PAO data set and 4.0×10^{19} eV for the AGASA data set, respectively. The merits of taking a higher value of energy cut for UHECR data in the analysis of positional correlations with astrophysical objects are 1) we can minimize the deflection due to the galactic and extragalactic magnetic fields; 2) we can reduce the diffuse isotropic components. The diffuse isotropic components may come from the contributions of our galaxy and far distant astrophysical object. We can reduce these contribution by taking the energy cut above the GZK cutoff, restricting possible sources within the GZK radius which is around 100 Mpc. Of course, the drawback is that we have a smaller number of data, which reduces the statistical power. So we need to compromise. Here, we apply the energy cut $E \geq E_c = 5.7 \times 10^{19}$ eV for both data sets. With this energy cut, we have 27 UHECR events from PAO and 23 UHECR events from AGASA. These are shown in FIG. 2.

The detector array does not cover the sky uniformly and we must consider its efficiency as a function of the arrival direction. It depends on the location and the characteristics of the detector array. Here we consider only the geometric efficiency which is determined by the location and the zenith angle cut of the detector array. Then the exposure function h depends only on the declination δ ,

$$h(\delta) = \frac{1}{\pi} [\sin \alpha_m \cos \lambda \cos \delta + \alpha_m \sin \lambda \sin \delta], \quad (4)$$

where λ is the latitude of the detector array, θ_m is the zenith angle cut, and

$$\alpha_m = \begin{cases} 0, & \text{for } \xi > 1, \\ \pi, & \text{for } \xi < -1, \\ \cos^{-1} \xi, & \text{otherwise} \end{cases} \quad \text{with } \xi = \frac{\cos \theta_m - \sin \lambda \sin \delta}{\cos \lambda \cos \delta}.$$

The PAO site has $\lambda = -35.20^\circ$ and the zenith angle cut of the data is $\theta_m = 60^\circ$. The AGASA site has $\lambda = +35.78^\circ$ and the zenith angle cut of the data is $\theta_m = 45^\circ$.

B. The Simple AGN Model for UHECR Sources

Now we consider a hypothesis that all or a certain fraction of UHECR with energy above a certain energy cut E_c are originated from the AGN within a certain distance cut d_c .

For the correlation analysis, we use AGN listed in the Véron-Cetty and Véron (VCV) catalog. The 12th edition of VCV catalog contains 108,080 quasars ($M < -23$), BL Lacertae

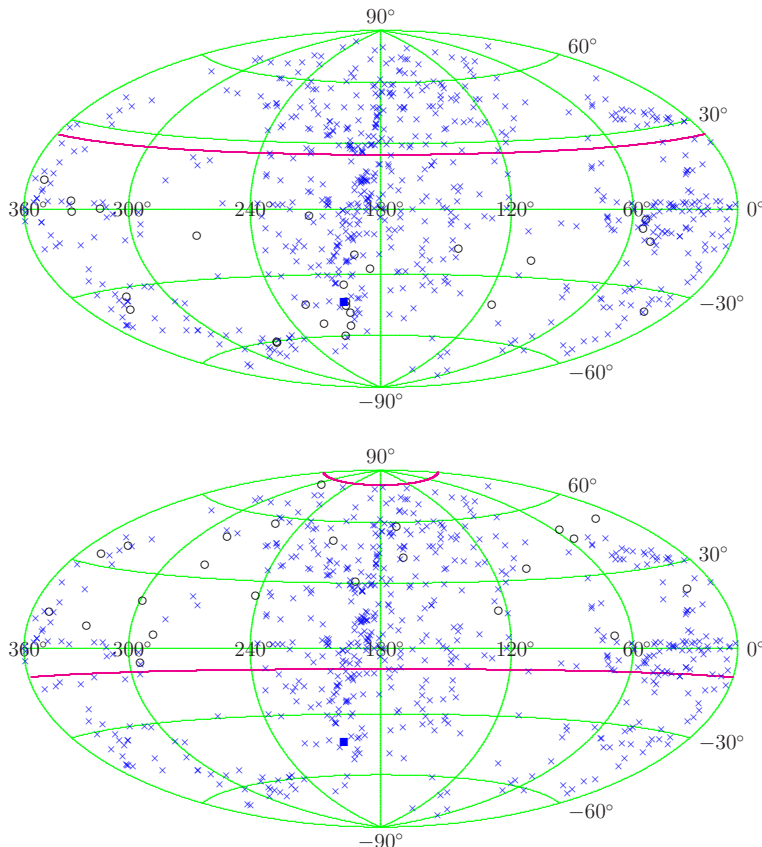


FIG. 2. Skymaps of the arrival directions of UHECR, represented by black circles (\circ), with energy $E \geq 5.7 \times 10^{19}$ eV observed by PAO (upper panel) and AGASA (lower panel) in the equatorial coordinates plotted using the Hammer projection. The solid red lines are the boundaries of the sky covered by PAO and AGASA experiments. The blue crosses (\times) represent the locations of AGN with distance $d \leq 100$ Mpc from the VCV catalog. The blue square (\blacksquare) shows the location of Centaurus A.

objects and AGN ($M > -23$) [20]. The catalog includes a variety of contents of each object, for example, the equatorial coordinates, magnitude, color index, redshift factor and so on. The catalog may not be a complete list of AGN we need. But we believe it covers enough number of AGN so that the statistical analysis will yield the useful information.

Because we apply the energy cut to UHECR data which is higher than the GZK cutoff, most of probable sources of them are expected to lie within the GZK radius. With this fact in mind and for the comparison with Refs. [3, 4], we pick up the AGN with the distance less than or equal to 100 Mpc (corresponding to the redshift $z \leq 0.024$) for the correlation test. The original number of AGN within 100 Mpc in the VCV catalog is 694. This includes 7 AGN with zero redshift, which are problematic to be included in our analysis. Thus, we eliminate these seven AGN from our AGN data set and the remaining 687 AGN will be used in our analysis. We show their locations in FIG. 2.

The UHECR luminosity would vary AGN by AGN in general. We now have a unified picture of AGN as the supermassive black hole surrounded by accreting materials. It is also known that the efficient particle acceleration can take place in the vicinity of the black hole and in the jet up to energies above 10^{19} eV through several different mechanisms [40].

However, it is still difficult to infer or to model the expected UHECR fluxes of all AGN due to limited measurements done so far and theoretical uncertainties. Thus, without a priori information, we assume that all AGN have the equal UHECR luminosity. Then, the UHECR flux from each AGN is just inversely proportional to the square of the distance to it.

We are considering AGN as the point sources of UHECR. However, the trajectories of UHECR are bent by intervening magnetic fields. Thus, the arrival directions of UHECR deviate from the exact AGN positions. (We also need to consider the uncertainty coming from the limitation of the angular resolutions of detector arrays.) To take this effect into account, we consider AGN as the smeared sources of UHECR. The smearing effect also varies AGN by AGN as well as UHECR by UHECR. But, for simplicity, we assume that all AGN are smeared sources having gaussian flux distribution about the locations with a common angular width θ_s , called the smearing angle. Here, the smearing angle, θ_s , is taken to be a free parameter. Semi-analytic analysis and numerical simulations of large scale structure formation indicated that the deflection of UHECR with $E \geq 4.0 \times 10^{19}$ eV is at best $2^\circ \sim 3^\circ$ [41, 42]. However, we take 6° as a fiducial value of θ_s to get the rather conservative constraint on the simple AGN model [10].

Now the UHECR flux distribution of each AGN is given by

$$f_i(\theta) = \frac{L}{4\pi d_i^2} \cdot \frac{e^{-(\theta/\theta_s)^2}}{\pi\theta_s^2}, \quad (5)$$

where L is the common UHECR luminosity, d_i is the distance to the AGN, and θ is the angular distance from the AGN position. The value of L is related to the total flux of UHECR, which we do not address here. Its precise value is not important for our purpose because it is equal for all AGN and our test compares the *normalized* probability distributions of UHECR events over the sphere.

The UHECR with energy above the energy cut $E_c = 5.7 \times 10^{19}$ eV still can come from the sources lying outside the distance cut $d_c = 100$ Mpc. The fraction of UHECR with $E \geq E_c$ coming from the sources with $d \leq d_c$ can be estimated as a function of E_c and d_c by solving the cosmic ray propagation equation. We denote this fraction as f_0 . For $E_c = 5.7 \times 10^{19}$ eV and $d_c = 100$ Mpc, the estimated value is $f_0 \approx 0.7$ [8].

In the simple AGN model considered here, we assume that the fraction f of observed UHECR with $E \geq E_c$ are originated from the AGN within the distance d_c and the remaining fraction $1 - f$ from isotropic background contributions. We call f the AGN fraction and treat it as a free parameter of the model, while its fiducial value is taken to be $f = f_0$. In FIG. 3, we show the distributions of the UHECR arrival directions expected from the simple AGN model with $f = 1$ and $f = 0.45$ as observed by PAO.

IV. THE CORRELATION OF AGN AND UHECR DATA

To illustrate our statistical methods, we take the set of selected AGN as our reference set and analyze the correlation between AGN and the arrival directions of UHECR by using the CADD method.

In FIG. 4 we compare the cumulative probability distribution (CPD) of CADD between the selected AGN (with $d \leq 100$ Mpc) and the arrival directions of UHECR from PAO data (with $E \geq 5.7 \times 10^{19}$ eV) with those expected from the simple AGN model which

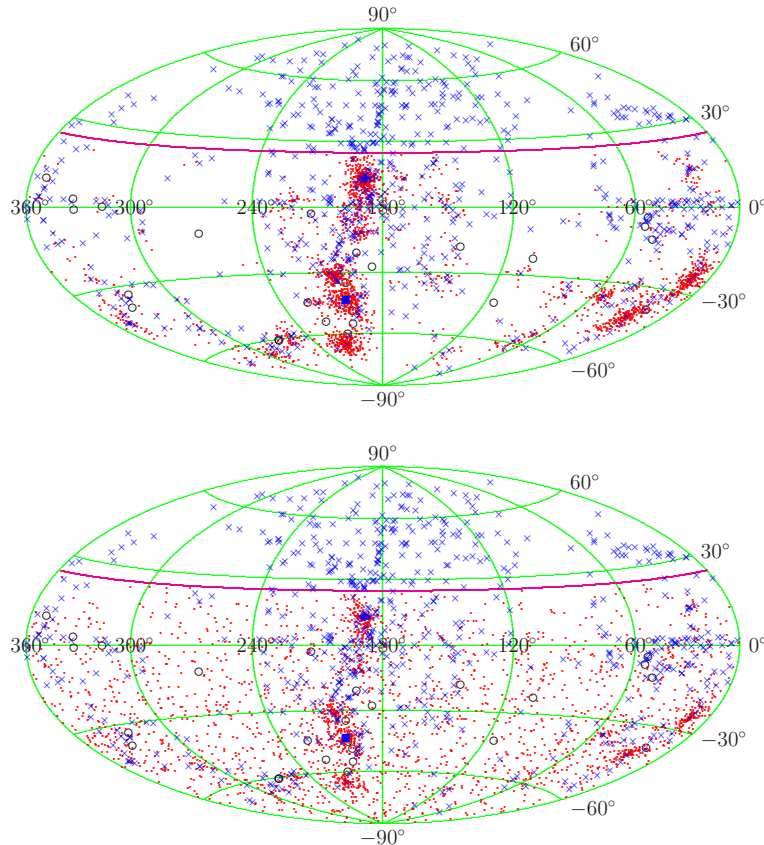


FIG. 3. The distributions of simulated UHECR arrival directions (2700 events, represented by red dots (.)) obtained from the simple AGN model with $f = 1$ (upper panel) and $f = 0.45$ (lower panel) in PAO case. Mapping and other symbols are same as in FIG. 2.

is obtained through Monte-Carlo simulations. Because the KS test is reparametrization invariant, we use the variable $x = \cos \theta$ instead of the angular distance θ in the horizontal axis. The CPD for the PAO data is the black line. The green line represents the CPD for the isotropic distribution (corresponding to $f = 0$) of UHECR and the blue and red lines represent the CPDs for the simple AGN model with a smearing angle of 6° for both and the source fraction $f = 1$ and $f = 0.45$, respectively. For comparing two different cumulative distribution functions $S_{N_1}(x)$ and $S_{N_2}(x)$, the KS statistic is [43]

$$D = \max |S_{N_1}(x) - S_{N_2}(x)|, \quad (6)$$

thus it can be directly read off from the CPDs. From the KS statistic D of CADD, the probability that the PAO data are yielded from the given model is given approximately by

$$\text{Probability} = Q_{\text{KS}} \left(\left[\sqrt{N_e} + 0.12 + 0.11/\sqrt{N_e} \right] D \right), \quad (7)$$

where $Q_{\text{KS}}(\lambda) = 2 \sum_{j=1}^{\infty} (-1)^{j-1} e^{-2j^2 \lambda^2}$ and N_e is the effective number of data points, $N_e = N_1 N_2 / (N_1 + N_2)$. When the number of observed UHECR events is N_o and the number of AGN is M , $N_1 = N_o M$ for CADD, $N_1 = N_o(N_o - 1)/2$ for AADD, and $N_1 = N_o$ for FEVD. For N_2 , we replace N_o with N_s , the number of simulated UHECR events. We compare the observed distribution, say S_{N_1} , with the expected distribution S_{N_2} , which is obtained

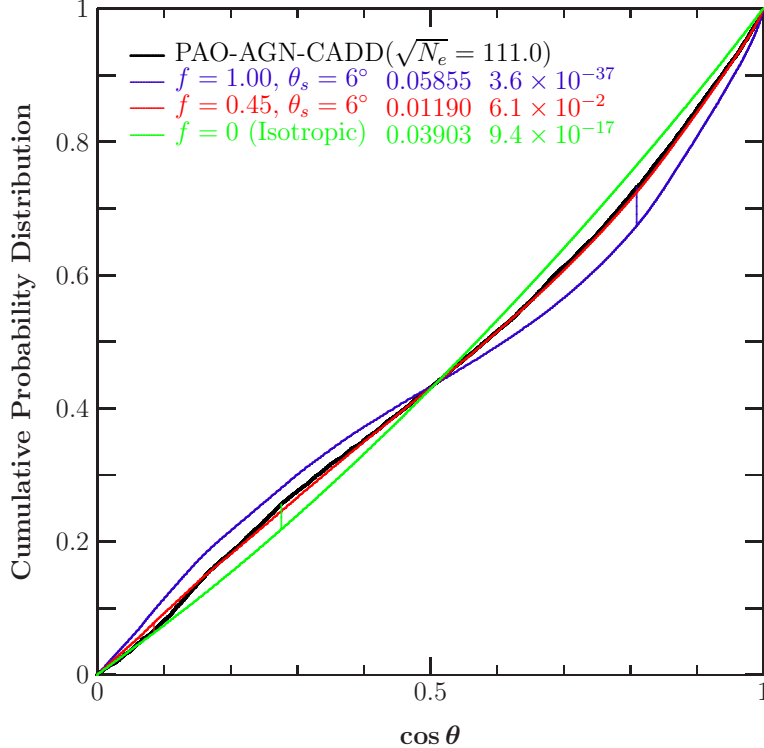


FIG. 4. The cumulative probability distributions of CADD using the AGN reference set. The black line is for the observed PAO data, the green line for the isotropic distribution, and the blue and red lines for the simple AGN model with a smearing angle $\theta_s = 6^\circ$ and a source fraction $f = 1$ and $f = 0.45$, respectively. The vertical bars represent the KS statistics which are the maximum differences between two CPDs. The numbers in two right columns in the legend are the KS statistics and the probabilities that the observed distribution of PAO arrival directions is obtained from the simple AGN models.

from the model through simulations. The expected distribution can be made accurate by increasing the number of simulated UHECR events N_s . We set $N_s = 10^6$ for CADD and FEVD, and $N_s = 10^4$ for AADD for the reason of practical computation, that is, it gives the accuracy sufficient for our purpose in reasonable computation time, though a little bit of fluctuations in calculating probabilities still remain. Since N_s is much larger than N_o , $N_e \approx N_1$. The values of probability are shown in the upper-left corner in the figure. We note that the CPD itself is also useful for comparing the correlations. The steep rise of CPD near $\cos\theta = 1$ means the strong correlation at small angles. Comparing the CPDs, we see that the PAO data are much more correlated with the AGN at small angles than the simple isotropic distribution. The probability that the PAO data result from the isotropic distribution is about 10^{-16} . But the PAO data are not correlated with AGN as much as required by the simple AGN model with $f = 1$ and a small smearing angle. For example the probability that the PAO data are yielded wholly from the AGN (that is $f = 1$) with the smearing angle of 6° is 2.1×10^{-37} , which is extremely small.

We can do the same kind of analysis now by using the FEVD or the AADD. Different methods will give different probabilities for the same hypothesis, showing the difference in their discriminating powers. Thus, we combine three methods together to make better and reliable conclusions.

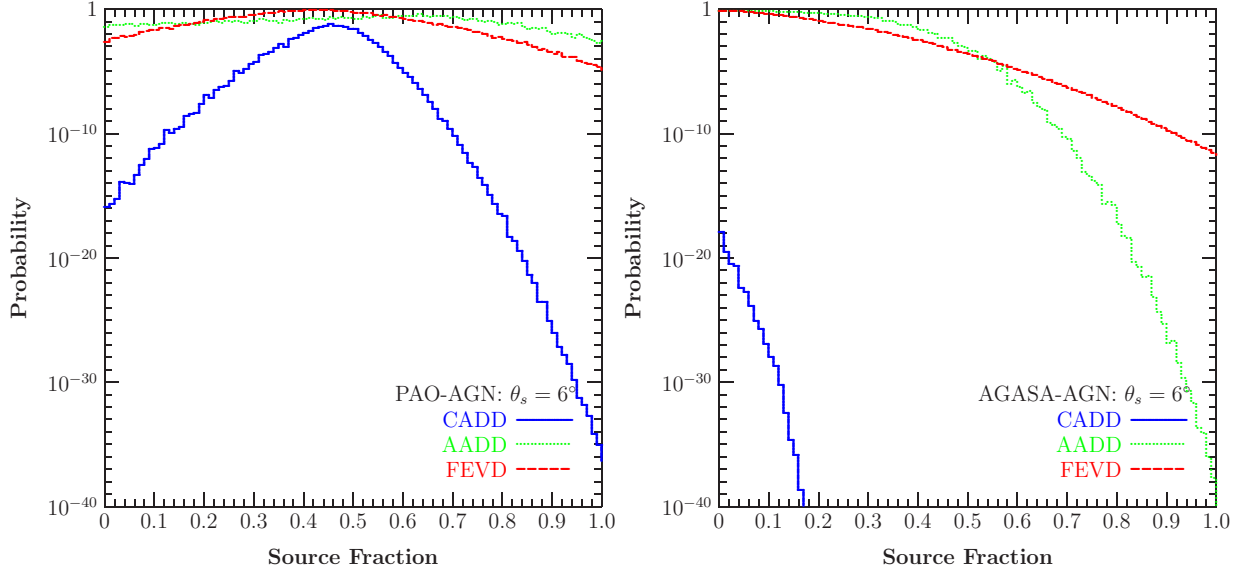


FIG. 5. Source fraction (f) dependence of probabilities from three different analysis methods for the AGN and the PAO data.

A. Dependence on the AGN fraction and the smearing angle

Now we examine the simple AGN model in detail. Even though we introduced two parameters f and θ_s for quite different motivations, their effects on the distribution of UHECR arrival directions are not clearly separated because both reducing f and making θ_s larger will make the distribution rather isotropic. Let us first consider the source fraction dependence of the distribution. In the simple AGN model, while f is the fraction of UHECR coming from the selected AGN, the remaining $1 - f$ is the fraction of UHECR coming from the isotropic background. In FIG. 5, we showed the f dependence of probabilities, obtained by using CADD, FEVD, and AADD methods, that the PAO data set and the AGASA data set are obtained from the simple AGN model (with AGN within 100 Mpc) with the smearing angle 6° . The CADD method gives the most stringent constraint and it clearly excludes both limits of $f = 0$ (complete isotropy) and $f = 1$ (all UHECR from selected AGN). However, a striking result is that for the PAO data set the probability is peaked at $f \approx 0.45$ with a value 0.064. In the previous section, we mentioned that the energy cut of UHECR $E = 5.7 \times 10^{19}$ eV and the distance cut of AGN $d_c = 100$ Mpc roughly determines the fraction of contribution from the inside of the distance cut, $f \approx 0.7$. The peak is away from this value and we need more isotropic components to get the best probability. For the fixed value of $f \approx 0.7$, a good probability can be achieved by increasing the smearing angle, as discussed below.

For the AGASA data set, we don't see any correlation with AGN. Rather, the FEVD and AADD methods indicate that the observed AGASA data are consistent with complete isotropy, even though the CADD method still gives maximum but tiny probability.

The smearing angle θ_s in the simple AGN model is a free parameter, though setting it a large value may need some justification, such as the existence of very strong intergalactic magnetic fields. We also examine the smearing-angle dependence of the correlation analysis and show the results in FIG. 6 and 7. Here again the CADD method plays a main role, while the FEVD method is sensitive at small smearing angles. As the smearing angle increases,

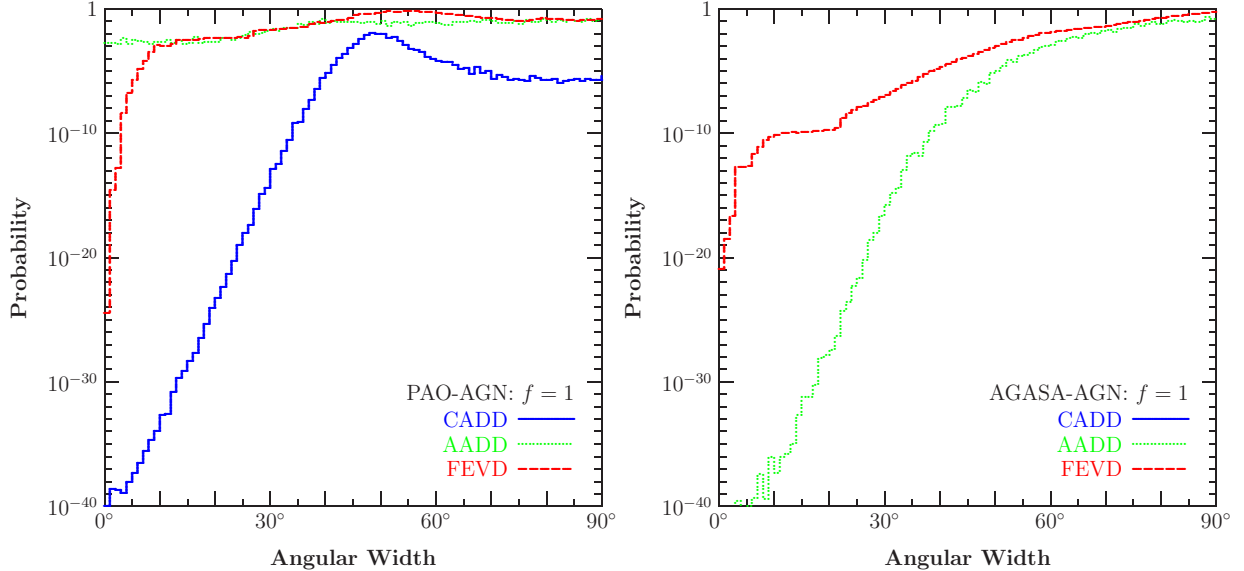


FIG. 6. Smearing-angle (θ_s) dependence of probabilities from three different analysis methods for the PAO data (left) and the AGASA data (right) with the source fraction $f = 1$. In the AGASA result (right), the CADD line is not seen because it lies below 10^{-40} .

the distribution of the arrival directions tends to be isotropic. In the above, we saw that the addition of isotropic component to some extent improves the probability for the PAO data set. Thus, we expect that increasing the smearing angle will also bring an improvement. For $f = 1$ (all UHECR from selected AGN), this happens for a rather large value of the smearing angle and the probability is peaked at $\theta_s = 48^\circ$ with a value 0.016 (See the left panel of FIG. 6). For $f = 0.7$, which is the reference value for $E_c = 5.7 \times 10^{19}$ eV and $d_c = 100$ Mpc, the peak value is 0.019 at $\theta_s = 36^\circ$ (See the left panel of FIG. 7). If we set $f = 0.45$, the small smearing angle is preferred (See the right panel of FIG. 7).

B. Dependence on Distance-Bin

In the above correlation analysis, the number of observed UHECR is much smaller than the number of AGN. Thus, only some subset of AGN can actually be responsible for observed UHECR. Therefore, it is legitimate to classify AGN in some way to narrow down the possible sources of UHECR among them. Unfortunately, we don't have yet plausible criteria to classify AGN into possible UHECR sources and not. This is the reason why we included all AGN within a distance cut assuming the equal UHECR luminosity for all AGN in the previous analysis.

Now we may consider a sophisticated hypothesis that AGN with certain properties or within a certain region are actually responsible for the UHECR. As for the first and simple-minded step toward this direction, we consider distance binning, though we don't have any reasonable motivation yet except the exploratory analysis of the UHECR data. FIG. 8 shows the probabilities by three analysis methods within the simple AGN model with equally sized 20 Mpc distance-binning, for which we set $f = 1$, $\theta_s = 6^\circ$ and use only those AGN within each bin as UHECR sources. While we have tried several different bin sizes of 10, 20 Mpc etc., here we present the results for the 20 Mpc bin size because it gives most interesting

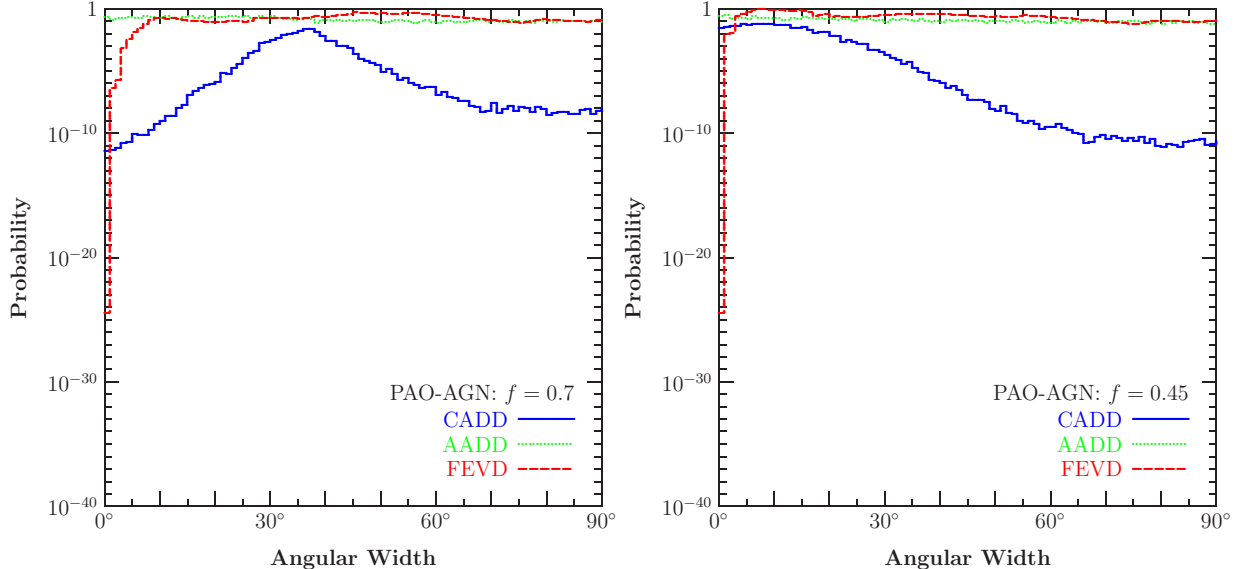


FIG. 7. Smearing-angle (θ_s) dependence of probabilities from three different analysis methods for the PAO data with the source fraction $f = 0.7$ (left) and $f = 0.45$ (right).

results. For the AGASA data, nothing interesting happens. But, quite interestingly, we find that with the PAO data the bin with $40 \text{ Mpc} < d \leq 60 \text{ Mpc}$ gives remarkable probabilities for all three methods, and this is manifestly seen with the bin size of 20 Mpc. We may further try a single bin of arbitrary size to find the best AGN set for the PAO data. We find that the probability is maximized with the value $P_{\text{CADD}} = 0.27$ when we select AGN within $41 - 63 \text{ Mpc}$ bin. For the comparison with FIG. 2, FIG. 9 shows the same skymap as the upper panel in FIG. 2 but for the AGN in the distance bin $40 \text{ Mpc} < d \leq 60 \text{ Mpc}$. We report this result just because it looks interesting, though it seems difficult to make an appropriate interpretation yet.

V. DISCUSSION AND CONCLUSION

The previous analysis of the correlation between AGN and the arrival directions of UHECR done by PAO group was based on the number of UHECR events correlated with AGN, where ‘correlated’ means that UHECR lie within a certain angular distance ψ from AGN [3, 4]. They used the data sets, AGN with $d \leq 71 \text{ Mpc}$ and UHECR with $E \geq 5.7 \times 10^{19} \text{ eV}$, and the angular distance $\psi = 3.2^\circ$ which minimize the probability of the null hypothesis that the distribution of UHECR arrival directions is isotropic. Under this condition, they found 20 out of 27 UHECR events are correlated with AGN. The chance probability that this number occurs from the isotropic distribution is 4.6×10^{-9} . Instead of the correlated UHECR events, our methods compares the reduced one-dimensional distributions, CADD, AADD, and FEVD of the observed UHECR events and the expected ones from the model, or the hypothesis. When applied to the same data sets, our methods yield the chance probabilities $P_{\text{CADD}} \approx 2.1 \times 10^{-9}$, $P_{\text{AADD}} \approx 4.9 \times 10^{-2}$, and $P_{\text{FEVD}} \approx 2.5 \times 10^{-3}$ from the isotropic distribution. These show that CADD is much better than FEVD and AADD in revealing anisotropy of the PAO data. The CADD method gives the result consistent with that of the PAO group. The advantage of using CADD is that we can avoid the

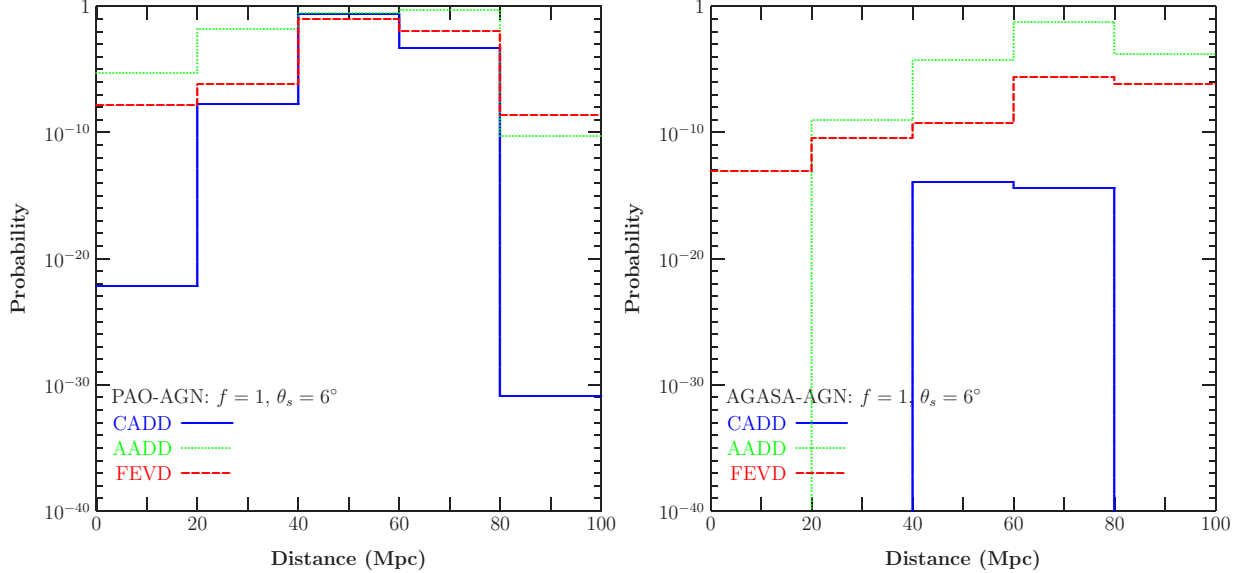


FIG. 8. Distance-bin dependence of probabilities for the PAO data (left panel) and the AGASA data (right panels) with the distance bin size of 20 Mpc.

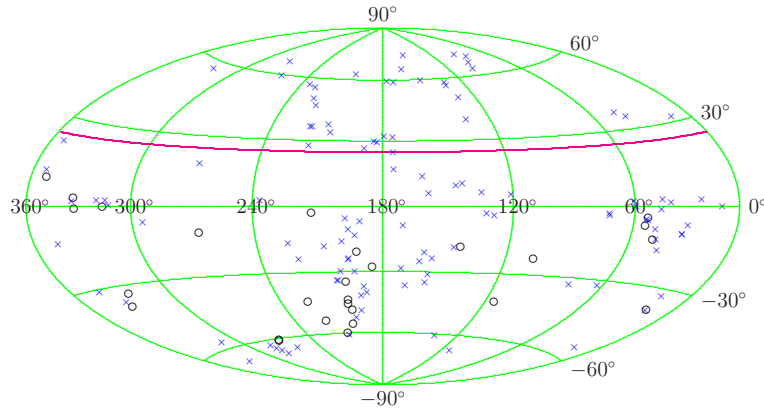


FIG. 9. Skymap of AGN with $40 \text{ Mpc} < d \leq 60 \text{ Mpc}$ and the arrival directions of UHECR with $E \geq 5.7 \times 10^{19} \text{ eV}$ observed by PAO.

arbitrariness in tuning the size of ψ to minimize the chance probability.

Even though the null hypothesis of isotropic distribution can be ruled out in these ways, it does not directly test the correlation between AGN and UHECR. This fact was already pointed out in Ref. [23]. For the direct test of correlation, we must set up an alternative hypothesis that AGN are the sources of UHECR. The null hypothesis we adopted is rather simple-minded in that all AGN listed in the catalog are treated as equal sources of UHECR. Our test reveals that the hypothesis that all UHECR with $E \geq 5.7 \times 10^{19} \text{ eV}$ observed by PAO come from AGN with $d \leq 71 \text{ Mpc}$ is also ruled out by the chance probability of $P_{\text{CADD}} = 1.3 \times 10^{-24}$. It says that the observed UHECR are more correlated with AGN than the simple isotropic distribution, but not sufficiently correlated with AGN as required by that hypothesis. Our result is consistent with that of Ref. [23].

In conclusion, we developed the statistical methods for comparing two sets of arrival directions of cosmic rays, in which the two-dimensional distribution of arrival directions is

reduced to the one-dimensional distributions such as CADD, AADD, and FEVD. Then the probability that the observed arrival direction distribution comes from the given hypothesis can be calculated by the standard one-dimensional KS statistic. We applied three methods together in combination to the analysis of correlation between UHECR and AGN to get improved and reliable conclusions. We used UHECR with energies above 5.7×10^{19} eV observed by PAO and AGASA, and AGN within the distance 100 Mpc listed in the 12th edition of VCV catalog. As our analysis showed, CADD is more useful than FEVD and AADD in testing the anisotropy and the correlation with AGN.

We set up the simple AGN model which assumes that all AGN within a chosen distance cut are the equal sources of UHECR having the same UHECR luminosity and smearing angle. For the PAO data, our methods exclude both limits that the observed UHECR are simply isotropically distributed and that they are completely originated from the selected AGN. However, we need to add the isotropic component to incorporate the contribution from the outside of the distance cut and the smearing effect due to the intergalactic magnetic fields. Increasing isotropic component either through the background contribution or through the large smearing effect improves the situation greatly and makes the AGN hypothesis for UHECR sources a viable one. But the required amount of the isotropic component is more than the estimated contribution from the outside of the distance cut. Thus, the rather large smearing angle is needed. We also point out that restricting AGN within the distance bin of 40–60 Mpc happens to yield a good probability without appreciable isotropic component and large smearing effect.

For the AGASA data, we don't find any significant correlation with AGN. Thus, as for the AGN hypothesis for the UHECR sources, we have quite different and even conflicting conclusions from PAO and AGASA experiments which mainly covers the southern sky and the northern sky, respectively. Of course, we cannot completely exclude the possibility that the observed correlation with AGN for the PAO data is just a mere chance. Now, the northern sky is being covered by Telescope Array (TA) experiment. We hope the UHECR data from TA will resolve this problem.

[Note Added] As this work is completed, PAO released the new data of UHECR [5]. Also new catalogs of AGN are available now [44, 45]. The results for these new data sets will be presented in a separate paper [46].

ACKNOWLEDGMENT

This research was supported by Basic Science Research Program through the National Research Foundation (NRF) funded by the Ministry of Education, Science and Technology (2009-0083563, 2010-0016307).

-
- [1] J. Abraham *et al.* [Pierre Auger Collaboration], “Observation of the suppression of the flux of cosmic rays above 4×10^{19} eV,” *Phys. Rev. Lett.* **101**, 061101 (2008) [arXiv:0806.4302 [astro-ph]].
 - [2] R. U. Abbasi *et al.* [HiRes Collaboration], “Observation of the GZK cutoff by the HiRes experiment,” *Phys. Rev. Lett.* **100**, 101101 (2008) [arXiv:astro-ph/0703099].

- [3] J. Abraham *et al.* [Pierre Auger Collaboration], “Correlation of the highest energy cosmic rays with nearby extragalactic objects,” *Science* **318**, 938 (2007) [arXiv:0711.2256 [astro-ph]].
- [4] J. Abraham *et al.* [Pierre Auger Collaboration], “Correlation of the highest-energy cosmic rays with the positions of nearby active galactic nuclei,” *Astropart. Phys.* **29**, 188 (2008) [Erratum-ibid. **30**, 45 (2008)] [arXiv:0712.2843 [astro-ph]].
- [5] P. Abreu *et al.* [Pierre Auger Observatory Collaboration], “Update on the correlation of the highest energy cosmic rays with nearby extragalactic matter,” arXiv:1009.1855 [Unknown].
- [6] H. Takami, T. Nishimichi and K. Sato, “Systematic Survey of the Correlation between Northern HECR Events and SDSS Galaxies,” arXiv:0910.2765 [astro-ph.HE].
- [7] A. J. Cuesta and F. Prada, “The correlation of UHECR with nearby galaxies in the Local Volume,” arXiv:0910.2702 [astro-ph.HE].
- [8] H. B. J. Koers and P. Tinyakov, “Testing large-scale (an)isotropy of ultra-high energy cosmic rays,” *JCAP* **0904**, 003 (2009). [arXiv:0812.0860 [astro-ph]].
- [9] H. Takami, T. Nishimichi, K. Yahata and K. Sato, “Cross-Correlation between UHECR Arrival Distribution and Large-Scale Structure,” *JCAP* **0906**, 031 (2009) [arXiv:0812.0424 [astro-ph]].
- [10] T. Kashti and E. Waxman, “Searching for a Correlation Between Cosmic-Ray Sources Above 10^{19} eV and Large-Scale Structure,” *JCAP* **0805**, 006 (2008) [arXiv:0801.4516 [astro-ph]].
- [11] R. S. Nemmen, C. Bonatto and T. Storchi-Bergmann, “A correlation between the highest energy cosmic rays and nearby active galactic nuclei detected by Fermi,” *Astrophys. J.* **722**, 281 (2010) [arXiv:1007.5317 [astro-ph.HE]].
- [12] Y. Y. Jiang, L. G. Hou, X. H. Sun, W. Wang and J. L. Han, “Do Ultrahigh Energy Cosmic Rays Come from Active Galactic Nuclei and Fermi γ -ray Sources?,” *Astrophys. J.* **719**, 459 (2010) [arXiv:1004.1877 [astro-ph.HE]].
- [13] N. Mirabal and I. Oya, “Correlating Fermi gamma-ray sources with ultra-high energy cosmic rays,” arXiv:1002.2638 [astro-ph.HE].
- [14] R. U. Abbasi *et al.*, “Search for Correlations between HiRes Stereo Events and Active Galactic Nuclei,” *Astropart. Phys.* **30**, 175 (2008) [arXiv:0804.0382 [astro-ph]].
- [15] R. U. Abbasi *et al.* [HiRes Collaboration], “Search for Cross-Correlations of Ultra-High-Energy Cosmic Rays with BL Lacertae Objects,” *Astrophys. J.* **636**, 680 (2006) [arXiv:astro-ph/0507120].
- [16] D. S. Gorbunov, P. G. Tinyakov, I. I. Tkachev and S. V. Troitsky, “Testing the correlations between ultra-high-energy cosmic rays and BL Lac type objects with HiRes stereoscopic data,” *JETP Lett.* **80**, 145 (2004) [*Pisma Zh. Eksp. Teor. Fiz.* **80**, 167 (2004)] [arXiv:astro-ph/0406654].
- [17] S. Singh, C. P. Ma and J. Arons, “Gamma-Ray Bursts and Magnetars as Possible Sources of Ultra High Energy Cosmic Rays: Correlation of Cosmic Ray Event Positions with IRAS Galaxies,” *Phys. Rev. D* **69**, 063003 (2004) [arXiv:astro-ph/0308257].
- [18] A. Smialkowski, M. Giller and W. Michalak, “Luminous infrared galaxies as possible sources of the UHE cosmic rays,” *J. Phys. G* **28**, 1359 (2002) [arXiv:astro-ph/0203337].
- [19] D. F. Torres, E. Boldt, T. Hamilton and M. Loewenstein, “Nearby quasar remnants and ultra-high energy cosmic rays,” *Phys. Rev. D* **66**, 023001 (2002) [arXiv:astro-ph/0204419].
- [20] M.-P. Véron-Cetty and P. Véron, “A catalog of quasars and active nuclei: 12th edition,” *Astron. Astrophys.* **455**, 773 (2006).
- [21] N. Hayashida *et al.*, “Updated AGASA event list above 4×10^{19} eV,” arXiv:astro-ph/0008102.
- [22] D. Harari, S. Mollerach and E. Roulet, “Kolmogorov-Smirnov test as a tool to study the distribution of ultra-high energy cosmic ray sources,” *Mon. Not. Roy. Astron. Soc.* **394**, 916

- (2009) [arXiv:0811.0008].
- [23] D. Gorbunov, P. Tinyakov, I. Tkachev and S. V. Troitsky, “Comment on ‘Correlation of the Highest-Energy Cosmic Rays with Nearby Extragalactic Objects’,” *JETP Lett.* **87**, 461 (2008) [arXiv:0711.4060 [astro-ph]].
- [24] O. E. Kalashev, B. A. Khrenov, P. Klimov, S. Sharakin and S. V. Troitsky, “Global anisotropy of arrival directions of ultra-high-energy cosmic rays: capabilities of space-based detectors,” *JCAP* **0803**, 003 (2008) [arXiv:0710.1382 [astro-ph]].
- [25] A. Cuoco, R. D. Abrusco, G. Longo, G. Miele and P. D. Serpico, “The footprint of large scale cosmic structure on the ultra-high energy cosmic ray distribution,” *JCAP* **0601**, 009 (2006) [arXiv:astro-ph/0510765].
- [26] M. Kachelriess and D. V. Semikoz, “Clustering of ultra-high energy cosmic ray arrival directions on medium scales,” *Astropart. Phys.* **26**, 10 (2006) [arXiv:astro-ph/0512498].
- [27] G. Sigl, F. Miniati and T. A. Ensslin, “Ultra-high energy cosmic ray probes of large scale structure and magnetic fields,” *Phys. Rev. D* **70**, 043007 (2004) [arXiv:astro-ph/0401084].
- [28] N. W. Evans, F. Ferrer and S. Sarkar, “The anisotropy of the ultra-high energy cosmic rays,” *Astropart. Phys.* **17**, 319 (2002) [arXiv:astro-ph/0103085].
- [29] P. Sommers, “Cosmic Ray Anisotropy Analysis with a Full-Sky Observatory,” *Astropart. Phys.* **14**, 271 (2001) [arXiv:astro-ph/0004016].
- [30] E. Waxman, K. B. Fisher and T. Piran, “The signature of a correlation between $> 10^{19}$ eV cosmic ray sources and large scale structure,” *Astrophys. J.* **483**, 1 (1997) [arXiv:astro-ph/9604005].
- [31] J. A. Peacock, *Mon. Not. Roy. Astron. Soc.* **202**, 615 (1983).
- [32] G. Fasano and A. Franceschini, *Mon. Not. Roy. Astron. Soc.* **225**, 155 (1987).
- [33] N. I. Fisher, T. Lewis, and B. J. J. Embleton, “Statistical Analysis of Spherical Data” (Cambridge University Press, 1987).
- [34] R. H. C. Lopes, I. Reid and P. R. Hobson, “A two-dimensional Kolmogorov-Smirnov test,” *PoS A CAT*, 045 (2007).
- [35] S. A. Metchev and J. E. Grindlay, “A two-dimensional Kolmogorov-Smirnov test for crowded field source detection: ROSAT sources in NGC 6397,” *Mon. Not. Roy. Astron. Soc.* **335**, 73 (2002) [arXiv:astro-ph/0204391].
- [36] R. U. Abbasi *et al.* [The High Resolution Fly’s Eye Collaboration (HIRES)], “Study of Small-Scale Anisotropy of Ultrahigh Energy Cosmic Rays Observed in Stereo by HiRes,” *Astrophys. J.* **610**, L73 (2004) [arXiv:astro-ph/0404137].
- [37] C. B. Finley and S. Westerhoff, “On the Evidence for Clustering in the Arrival Directions of AGASA’s Ultrahigh Energy Cosmic Rays,” *Astropart. Phys.* **21**, 359 (2004) [arXiv:astro-ph/0309159].
- [38] P. G. Tinyakov and I. I. Tkachev, “Correlation function of ultra-high energy cosmic rays favors point JETP Lett. **74**, 1 (2001) [*Pisma Zh. Eksp. Teor. Fiz.* **74**, 3 (2001)] [arXiv:astro-ph/0102101].
- [39] M. Takeda *et al.*, “Small-scale anisotropy of cosmic rays above 10^{19} eV observed with the Akeno Giant Air Shower Array,” *Astrophys. J.* **522**, 225 (1999) [arXiv:astro-ph/9902239].
- [40] F. M. Rieger, “Cosmic Ray Acceleration in Active Galactic Nuclei - On Centaurus A as a possible UHECR Source,” arXiv:0911.4004 [astro-ph.HE], and references therein.
- [41] K. Kotera and M. Lemoine, “The optical depth of the Universe for ultra-high energy cosmic ray scattering in the magnetized large scale structure,” *Phys. Rev. D* **77**, 123003 (2008) [arXiv:0801.1450 [astro-ph]].

- [42] K. Dolag, D. Grasso, V. Springel and I. Tkachev, “Constrained simulations of the magnetic field in the local universe and the propagation of UHECRs,” *JCAP* **0501**, 009 (2005) [arXiv:astro-ph/0410419].
- [43] W. H. Press, S. A. Teukolsky, W. T. Vettering, and B. P. Flannery, “Numerical Recipes” 3rd Ed. (Cambridge University Press, 2007).
- [44] A. A. Abdo and f. L. Collaboration, “The First Catalog of Active Galactic Nuclei Detected by the Fermi Large Area Telescope,” *Astrophys. J.* **715**, 429 (2010) [arXiv:1002.0150 [astro-ph.HE]].
- [45] See <http://heasarc.gsfc.nasa.gov/W3Browse/all/veroncat.html>.
- [46] Hang Bae Kim and Jihyun Kim, “Update of correlation analysis between active galactic nuclei and ultra-high cosmic rays,” in preparation.